



Nanostructures defined by the local oxidation of the ferromagnetic GaMnAs layer

J. Voves^{a,*}, Z. Šobáň^a, M. Janoušek^a, V. Komarnickij^a, M. Cukr^b, V. Novák^b

^a Department of Microelectronics, Faculty of Electrical Engineering, Czech Technical University in Prague, Technická 2, CZ-166 27 Praha 6, Czech Republic

^b Department of Surfaces and Interfaces, The Institute of Physics of the ASCR v.v.i., Cukrovarnická 10, CZ-162 53 Praha 6, Czech Republic

ARTICLE INFO

Article history:

Received 28 February 2008

Accepted 31 July 2008

Available online 30 September 2008

Keywords:

Ferromagnetic semiconductor

Atomic force microscopy

Local anodic oxidation

Magnetoresistance

ABSTRACT

The results of local anodic oxidation (LAO) on the thin GaMnAs layers are reported. The ferromagnetic GaMnAs layers were prepared by low-temperature molecular beam epitaxy (MBE) growth in a Veeco Mod Gen II machine. The LAO process was performed with the atomic force microscope (AFM) Smena NT-MDT placed in the sealed box with the controlled humidity in the range 45–80%. The oxide was grown in the semi-contact mode of the AFM. The sample was positively biased with respect to the AFM tip with the bias from 6 to 24 V. The conductive diamond-coated AFM tips with the radius 30 nm were utilized for the oxidation. The tip speed during the oxidation was changed from 400 nm/s to 1.5 μm/s. The tip force was also changed during the oxidation. The height of oxide nanolines increases with applied voltage from 3 to 18 nm. The width of these lines was approximately 100 nm at half-maximum. The magnetoresistance measurements of the sample with 1D lateral constriction by the LAO and the micromagnetic simulations of the structure with two lateral constrictions are presented.

© 2008 Elsevier Ltd. All rights reserved.

1. Introduction

The fabrication and study of nanoelectronic devices demand the modification of metals and semiconductors on the nanometer length scale. Key elements for more complex structures such as transistors are narrow conducting wires and tunneling barriers. On the nanometer scale, proximal probe-based instruments, in particular the scanning tunneling microscope (STM) and atomic force microscope (AFM), have proven successful not only to image surfaces but also to modify them. AFM is a well-known instrument used for surface topography measurements. The principle of the method lies in monitoring of the tip motion above the inspected surface. The tip is fixed on the end of the elastic cantilever, which is deflected by attractive and repulsive forces between the surface and the tip. The deflection of the cantilever is optically scanned. Various approaches have been used to generate patterns by means of the AFM useful for device fabrication: mechanically modifying a resist layer, which then acts as an etch mask for pattern transfer, local anodic oxidation (LAO) and subsequent use of the oxide as the etch mask, and maskless techniques, i.e., those directly affecting the material's electron system by the proximal probe itself. This can be done again

mechanically or by using the probe for locally inducing chemical reactions. Early work on STM and contact AFM-induced oxidation of Si was done by Dagata et al. [1]. If the substrate surface and the tip are electrically conductive and the tip is biased negatively to the surface, local oxidation proceeds under the tip (see Fig. 1). With this method it is possible to fabricate oxide lines of any shape. Height of these formations reaches several nanometers and their width at half of the maximum is about 100 nm. Oxide lines can be written to form desired patterns on the surface by translating the tip in a controlled fashion. Several research groups have demonstrated the viability of this technique in both contact and tapping AFM modes. However, when the LAO is performed in the contact mode, the tip apex tends to degrade readily since the tip stays in physical contact with the surface. This subsequently shortens the life-time of the tip and sacrifices the resolution of oxide patterns. For these reasons, the noncontact/tapping AFM mode is the most preferred to perform the LAO. The AFM tip oxidizes the surface and forms an energy barrier for electrons in a metal or in a heterostructure. The LAO patterning is broadly reported on Ti [2], Si [3] and GaAs layers [4,5]. Unsuccessful attempt has been realized with the LAO on the GaN layer [6].

This method could be advantageous, especially for laboratory experiments. The sample surface can be examined before the oxidation. Consequently, it is possible to create oxide lines on the selected location. Oxidation results can be immediately investigated. In this work, a conducting AFM tip is used in the tapping

* Corresponding author. Tel.: +420 2 2435 2861; fax: +420 2 2431 0792.

E-mail address: voves@fel.cvut.cz (J. Voves).

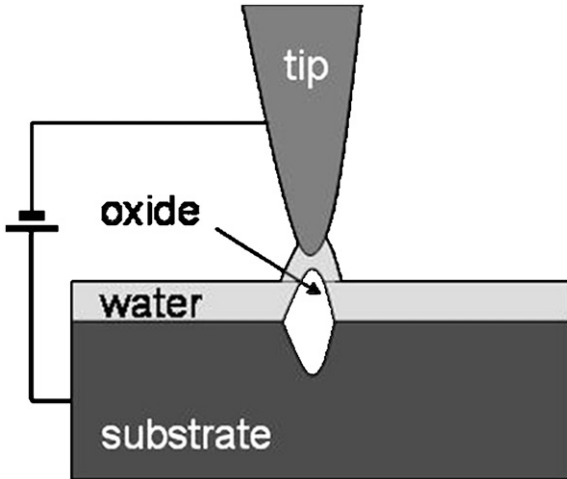


Fig. 1. LAO by the AFM tip.

mode to oxidize the GaMnAs surface producing nanometric constrictions in a thin ferromagnetic layer.

Several spin-valve and spin-filtering effects have been reported in the ferromagnetic nanostructures with the domain-wall pinning on the nanoconstrictions. The giant magnetoresistance (GMR) up to several hundred % is produced by the opposite magnetization of adjacent domain walls; the tunnel magnetoresistance (TMR) appears, when the constrictions are very narrow (below 10 nm), producing up to several thousand % [7]. Tunneling anisotropic magnetoresistance (TAMR) is present in the nanoconstricted structures with the strong spin-orbit coupling [8]. Application of the external magnetic field in the different directions produces both positive and negative magnetoresistance. Most of the nanoconstricted ferromagnetic structures are based on the GaMnAs layers patterned by the electron-beam lithography. The LAO by AFM is attracting attention because of its relatively low cost and high resolution. Very few reports are presented about the LAO on the ferromagnetic GaMnAs layers.

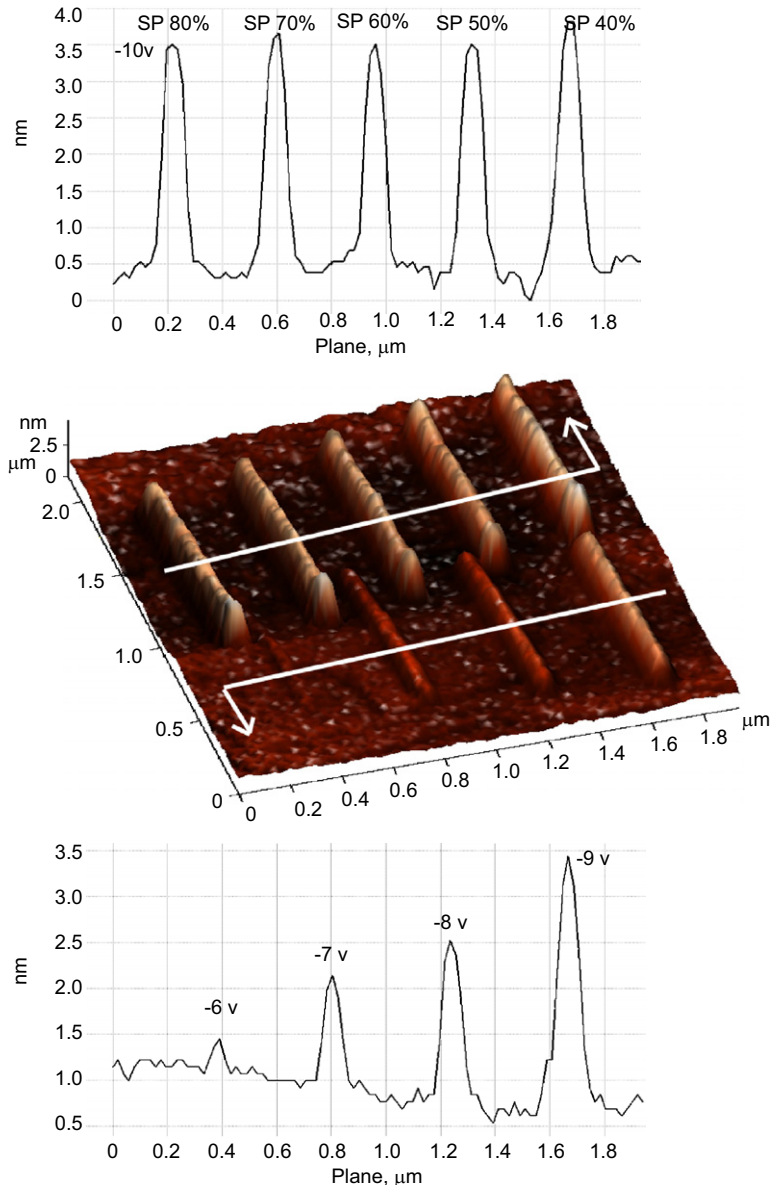


Fig. 2. The 3D picture of the oxide lines prepared by LAO in the GaMnAs layer using the semi-contact mode. Set point was lowered to 40% of the original value, increasing the force applied on the tip. Humidity was 75%. Tip velocity during LAO was 400 nm/s. Negative bias applied on the tip was 5, 6, 7, 8 and 9 V (from the left) for bottom lines and 10V for upper lines, where the tip force was varied without significant effect.

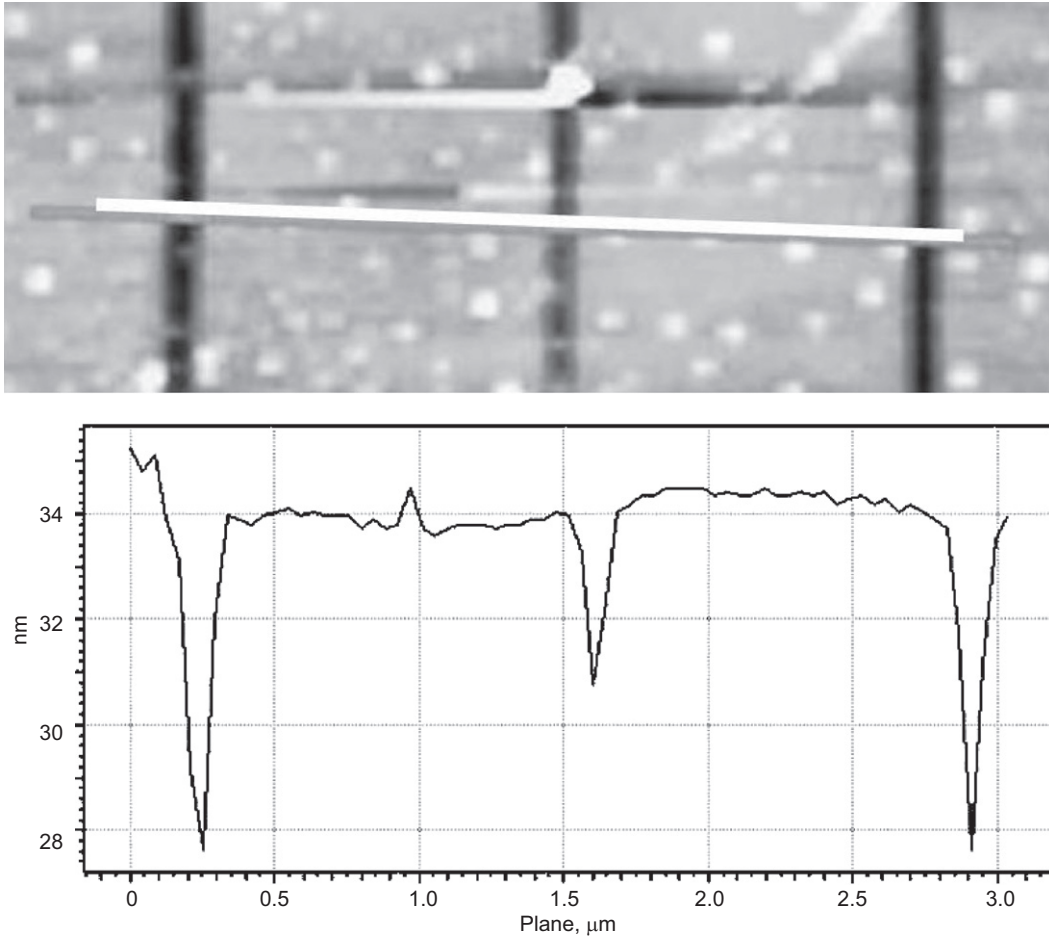


Fig. 3. The AFM picture of three oxide lines after etching in the HCl (upper) and the 1D profile along the white line (bottom).

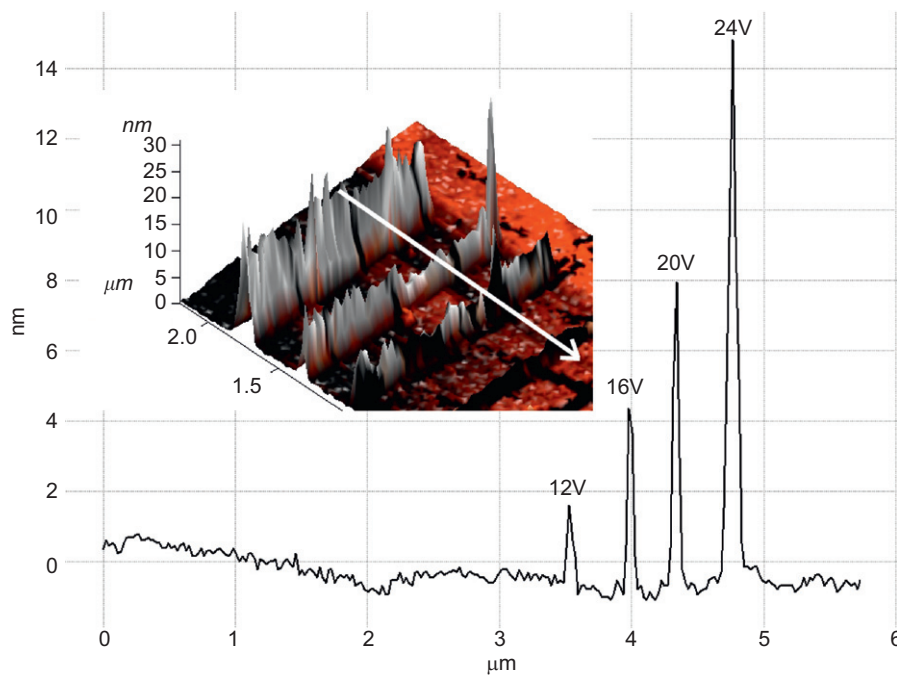


Fig. 4. The 1D profile of four oxide lines prepared by LAO in the GaMnAs layer with the external voltage source. Set point was lowered to 20% of the original value. Humidity was 50%. Tip velocity during LAO was 500 nm/s. Negative bias applied on the tip was 12, 16, 20 and 24 V. The 3D picture with a white 1D section line is in the insert.

2. Experimental

We present some results of our analysis of the LAO ability to produce lateral nanostructures in ferromagnetic semiconductor layers, namely in the thin GaMnAs layers grown by molecular beam epitaxy (MBE).

2.1. The MBE-grown GaMnAs layers

The layers were prepared by the low-temperature (LT) MBE growth in a Veeco Mod Gen II machine using As_4 beam. The oxidation was performed on several samples. The first structure consisted of a conventional high-temperature GaAs layer of about

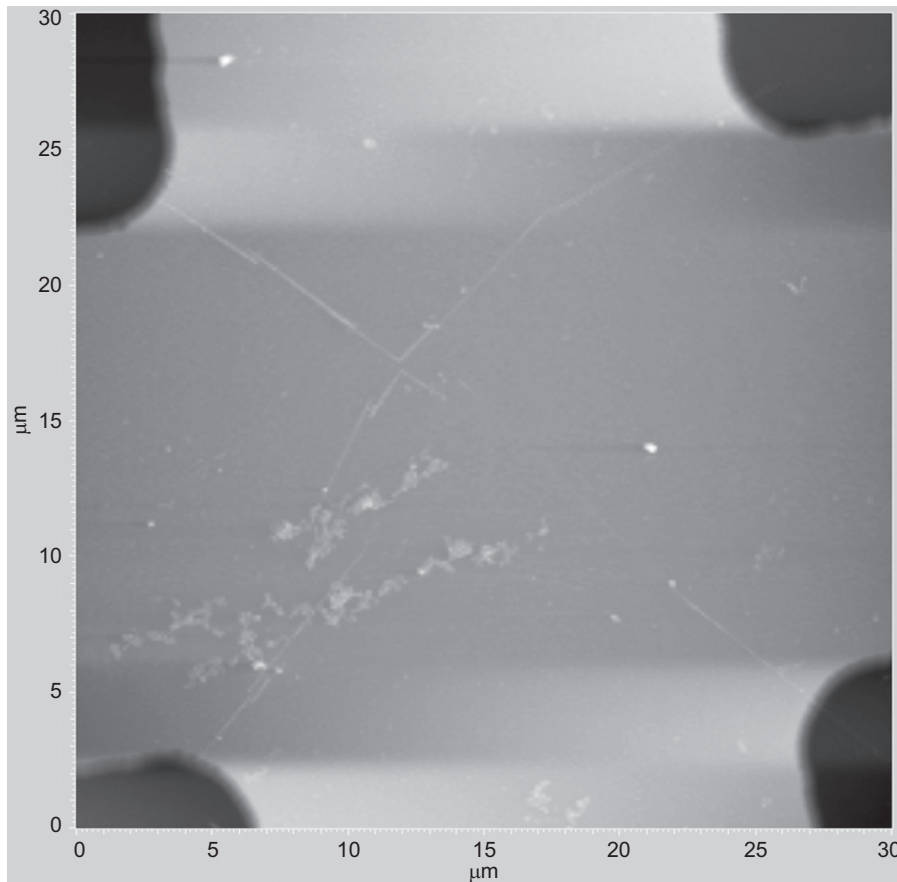


Fig. 5. The 1D constriction realized by two LAO lines in the center of the Hall bar.

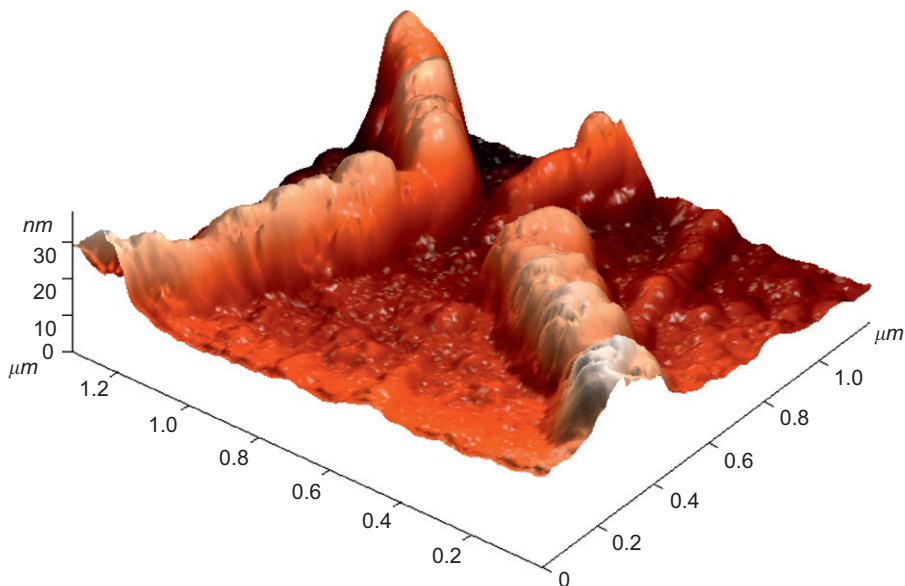


Fig. 6. AFM picture of the Hall bar center with 20 μm width.

200 nm thickness followed by a 5 nm LT GaAs layer and a 10 nm GaMnAs layer grown at 200 °C. The surface was atomically smooth with (1 × 2) reconstruction. The resulting Ga_{1-x}Mn_xAs layer with x_{Mn} = 7% had a T_C of about 55 K (as-grown) and about 150 K after annealing in air at 200 °C for 2 h. After annealing, the layer was conducting with the conductivity 200 Ω⁻¹ cm⁻¹. The second sample consisted of a 200 nm GaAs buffer layer followed by 4.5 nm a LT GaAs layer and 50 nm GaMnAs.

2.2. LAO parameters and results

Several parameters are required to be set correctly for the preparation of homogenous and sufficiently high oxide lines. Ambient humidity is very important for optimal oxidation process

[9]. Water condensates in a strong electrical field (10¹⁰ V/m) in between the tip and the sample. Due to capillary forces, the condensed water creates a water junction, which sequentially dissociates and acts as electrolyte for the following oxidation. The LAO process was performed with the AFM microscope Smena NT-MDT placed in a sealed box with controlled humidity in the range 45–80%. The oxide was grown in the semi-contact mode of the AFM. The sample was positively biased with respect to the AFM tip with the bias from 6 to 24 V. The conductive diamond-coated AFM tips with the radius 30 nm were used for the oxidation. The tip speed was changed from 400 nm/s to 1.5 μm/s during the oxidation. We used external voltage source to increase the applied bias above 10 V. The oxide lines prepared by LAO using internal voltage source are shown in Fig. 2. Set point was lowered

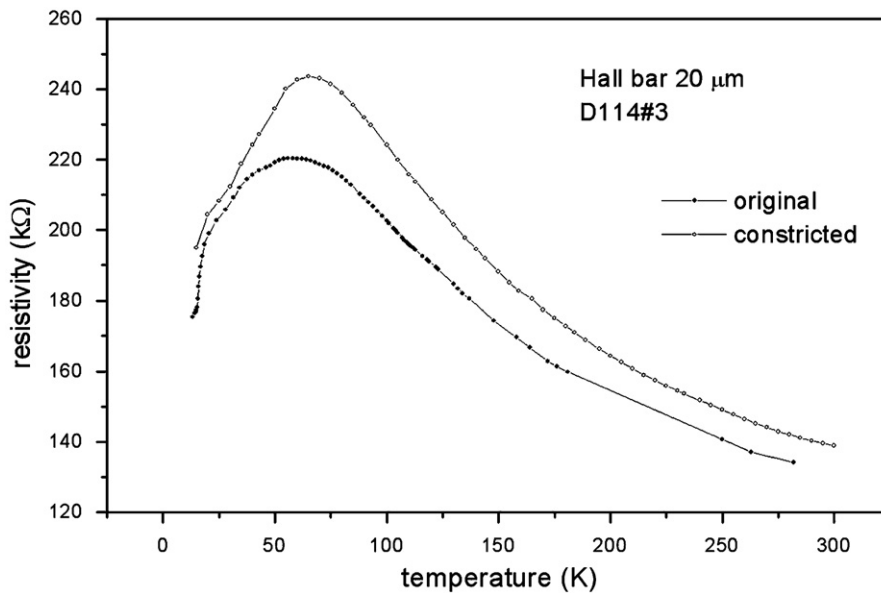


Fig. 7. Temperature dependence of the resistivity of the unconstricted and constricted sample.

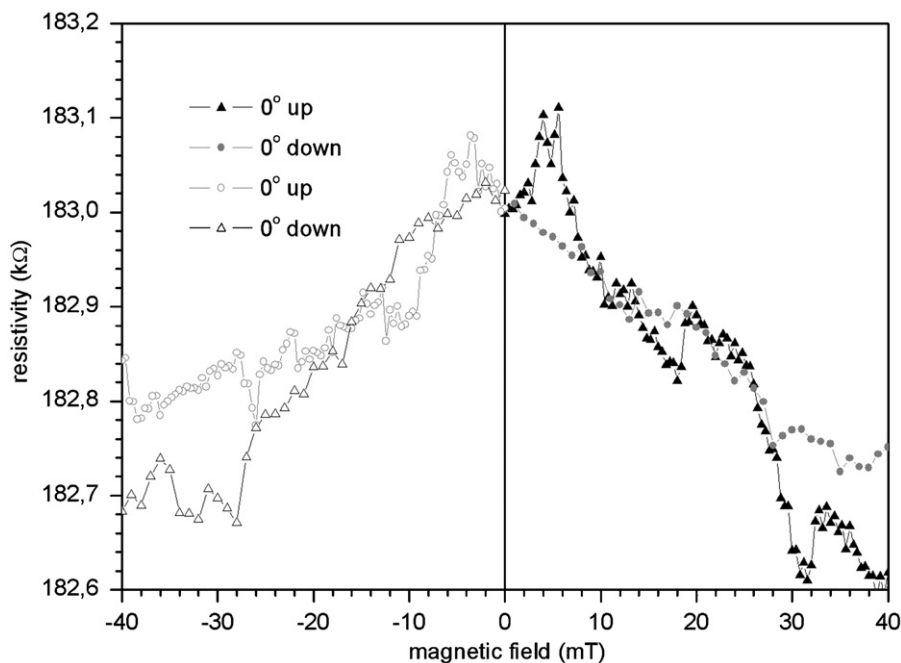


Fig. 8. The magnetoresistance of the constricted sample at 12 K. The in-plane magnetic field with parallel orientation with respect to the current flow direction was applied.

to 40% of the original value, increasing the force applied on the tip. Humidity was kept at 75%. Tip velocity during the LAO was 400 nm/s. Negative bias applied on the tip was 5, 6, 7, 8 and 9 V for bottom lines and 10 V for upper lines, where the tip force was varied without significant effect.

One sample was etched in the 3% HCl after oxidation. The resulting profile shows that the oxide depth is approximately the same as the line height above the surface (Fig. 3). Four oxide lines prepared by LAO with the external voltage source are shown in Fig. 4. The set point was lowered to 20% of the original value on the second sample. Humidity was 50%. Tip velocity during LAO was 500 nm/s. Negative bias applied on the tip was 12, 16, 20 and

24 V. The maximum height of the line is reached for the bias of 24 V (18 nm). Different optimal oxidation speed of 400 nm/s and ambient humidity of 75% have been found for each sample. No significant change in line height and homogeneity has been observed by the tip speed up to 1 $\mu\text{m/s}$.

2.3. Magnetoresistance results

We measured the first sample (10 nm GaMnAs layer), which was defined laterally by the optical lithography in the form of a Hall bar with a width of 20 μm . Then we made the 1D constriction by the LAO (Figs. 5 and 6). Temperature dependence of the

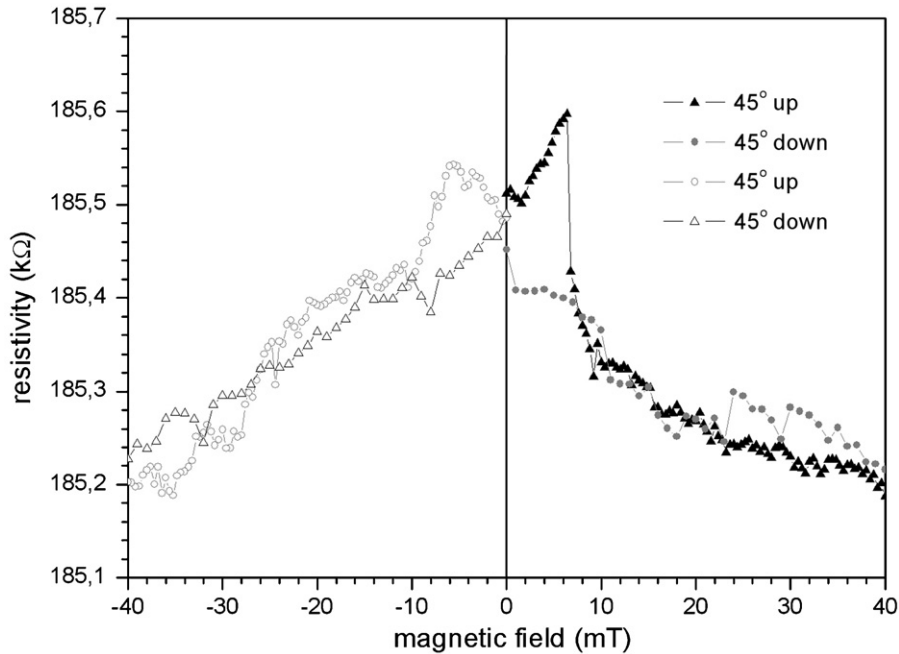


Fig. 9. The magnetoresistance of the constricted sample at 12 K. The in-plane magnetic field is turned by 45° to the current flow direction.

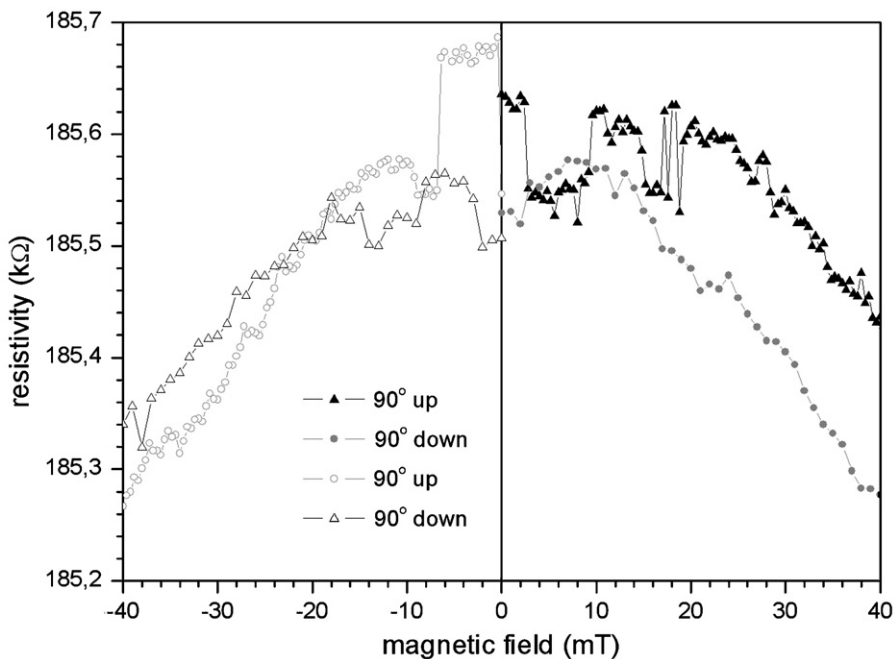


Fig. 10. The magnetoresistance of the constricted sample at 12 K. The in-plane magnetic field has the perpendicular orientation with respect to the current flow direction.

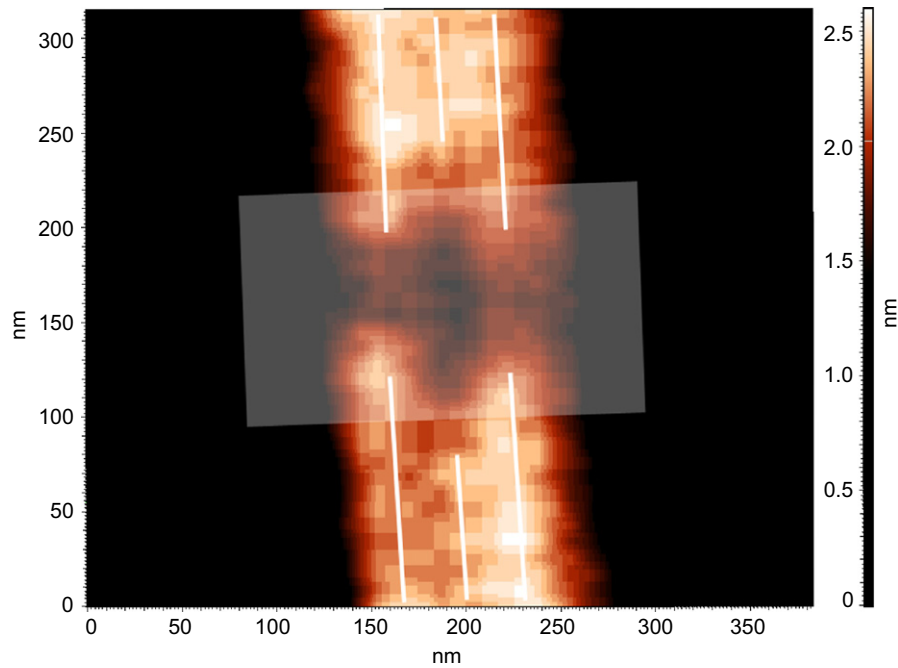


Fig. 11. The quantum dot produced by three interrupted lines with 38 nm spacing (white dotted lines). The simulated structure is defined by the white rectangle.

resistivity of the unconstricted and constricted sample is shown in Fig. 7. The resistivity drop below approximately 70 K is typical for the ferromagnetic semiconductor below the Curie temperature. The unconstricted sample shows no significant magnetoresistance effect up to magnetic field 120 mT at 12 K. The constricted sample has been measured in the in-plane magnetic field with different orientations with respect to the current flow direction. Relatively significant resistance maxima are observed in the all magnetic field orientations in the interval 0–10 mT by the magnetic field polarity reversal. In the orientation parallel to the current flow, the resistance has a double peak at 5 and 7 mT (Fig. 8). The peak at 7 mT is more evident by the orientation 45° (Fig. 9). In the perpendicular orientation, the resistivity is almost constant up to 7 mT and then sharply decreases (Fig. 10). These effects may be connected to domain-wall pinning at the constriction.

3. Simulation

Micromagnetic modeling can predict the magnetic behavior of materials on a short length scale of the order of nanometers. The individual magnetic moments will try to align themselves with an external field until the local energy minimum is reached. If the external field changes, the moments will rotate and the domain patterns change and move to a new configuration, corresponding to the new local energy minimum. The main focus of micromagnetism is to study the magnetization reversal process and the complex domain configurations, especially in thin films.

3.1. Micromagnetic simulator

The micromagnetic simulator SimulMag [10] is an easy-to-use PC-based magnetic design tool. The simulator allows one to simulate the system response of a magnetic device or circuit under the influence of external magnetic fields, currents or local field sources. The analysis is based on a collection of single-domain elements whose size and position can be specified by the

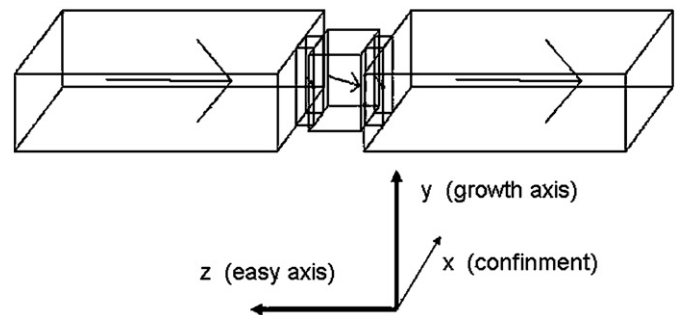


Fig. 12. The input structure for the micromagnetic simulation.

designer. The elements may be magnetic or nonmagnetic, a conductor or an insulator. The element's magnetic properties, such as magnetization, anisotropy, pinning fields and resistivity, must be specified or selected from a library of materials. Electrical circuits can be specified and currents applied. The elements interact through magnetostatic interactions and user-specified exchange interactions. The elements are arranged in groups to allow different structures to be built up and manipulated independently. Relative motion between the groups can be specified.

3.2. Simulated structure

A three-dimensional nanostructure with two constrictions was approximated by the rectangle-shaped oxide regions (rectangle in Fig. 11) constricting a thin GaMnAs layer on the semi-insulating GaAs buffer. Analysis of the structure in the external magnetic field with different orientation was performed by means of micromagnetic simulation software SimulMag. This simulator minimizes the Gibbs free energy of the micromagnetic system and uses semi-empirical models for GMR and AMR calculations. Input

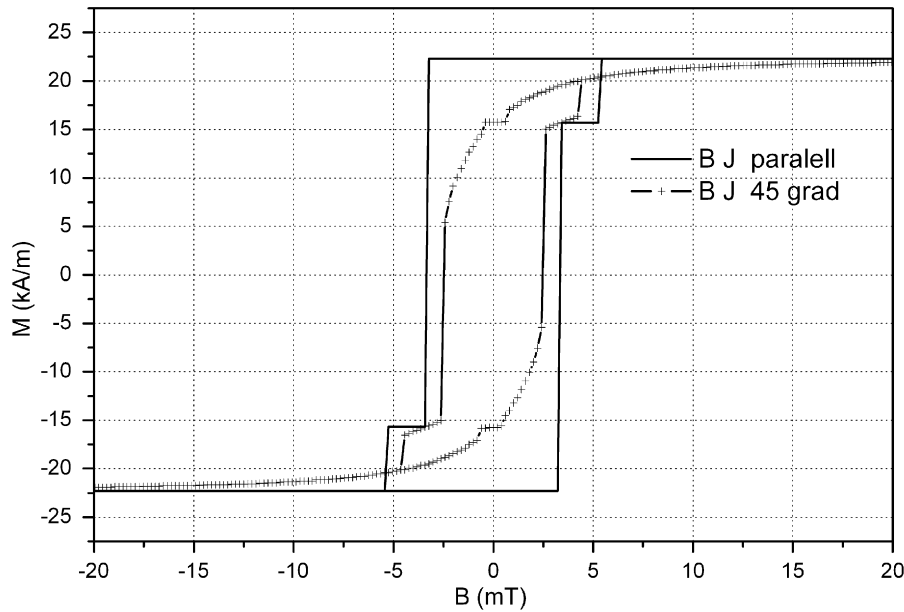


Fig. 13. Results of micromagnetic simulation by the external magnetic field. The field was changed from 30 to -30 mT and back. The resulting magnetization of the sample shows different levels of hysteresis with different in-plane field orientations (magnetic field B parallel to the current J and with the angle 45° between B and J).

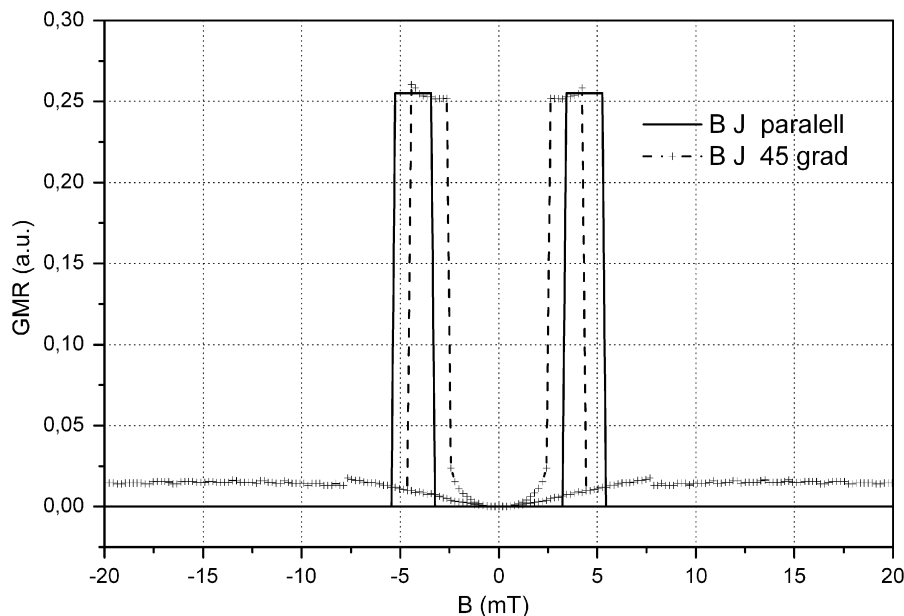


Fig. 14. The qualitative semi-empirical values of GMR with the same magnetic field orientations as in Fig. 12.

structure for the simulation is shown in Fig. 12. Magnetic easy axis was oriented along the z direction. The field was changed from 30 to -30 mT and back. We performed the static calculation of the structure magnetization. Saturated magnetization of the central quantum dot was chosen a little higher (40 kA/m) than in other regions (20 kA/m) to simulate the retarded switching of the central part magnetization during the magnetic field sweep. Resulting magnetization of the sample shows different levels of hysteresis with different field orientations (Fig. 13) as expected. The hysteresis loops show several nonlinearities due to retarded domain switching of the central dot by the magnetic field change. These nonlinearities produce sharp GMR changes, as shown in Fig. 14.

4. Conclusion

We analyzed the influence of the different conditions of the LAO by an AFM tip applied on the thin ferromagnetic GaMnAs layer. The maximum height of the obtained oxide lines was 18 nm by 24 V applied on the layer with respect to the AFM tip (Fig. 15). Oxidation speed of 400–500 nm/s and ambient humidity of 50–75% have been used. Optimal parameters should be found separately for each GaMnAs layer depending on its resistivity and surface quality. Nanostructures with the quantum dot in between the two constrictions were prepared. The analysis of the prepared nanostructure by means of micromagnetic simulation software SimuMag was performed. The simulation can help in the qualitative

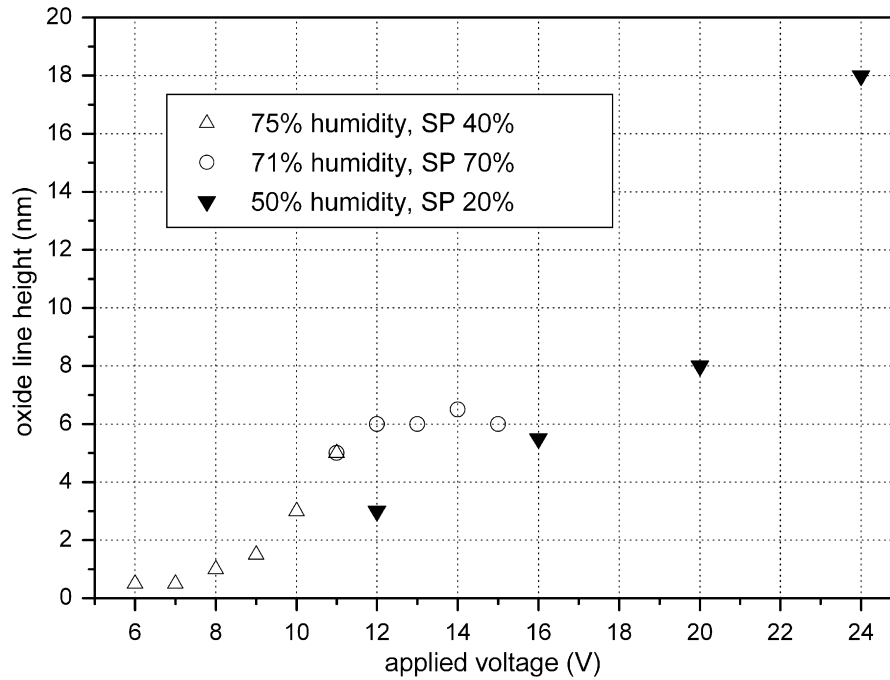


Fig. 15. Oxide line height vs. voltage applied on the AFM tip.

estimation of the ferromagnetic nanostructure behavior. The LT magnetotransport experiments have been realized on the structures with the single constriction. Measurements on the structures with two constrictions are started. The more pronounced magnetoresistance effect could be expected in these structures as predicted with the micromagnetic simulation and as measured on the structures prepared by the electron-beam lithography.

Acknowledgement

The work was supported by Grants no. 102/06/0381 GACR, no. KAN400100652 GA CAS and no. MSM 6840770014, The Ministry of Education, Czech Republic.

References

- [1] J.A. Dagata, J. Schneir, H.H. Harary, C.J. Evans, M.T. Postek, J. Bennett, *Appl. Phys. Lett.* 56 (1990) 2001.
- [2] B. Irmer, M. Kehrle, H. Lorenz, J.P. Kotthaus, *Appl. Phys. Lett.* 71 (1997) 1733.
- [3] J. Červenka, R. Kalousek, M. Bartošík, D. Škoda, O. Tomanec, T. Šíkola, *Appl. Surf. Sci.* 253 (2006) 2373.
- [4] R. Nemetudi, N.J. Curson, N.J. Appleyard, D.A. Ritchie, G.A.C. Jones, *Microelectron. Eng.* 57–58 (2001) 967.
- [5] U.F. Keyser, H.W. Schumacher, U. Zeitler, R.J. Haug, K. Eberl, *Appl. Phys. Lett.* 76 (2000) 457.
- [6] A. Pakes, et al., *J. Mater. Sci.* 38 (2003) 343.
- [7] C. Rüster, et al., *Phys. Rev. Lett.* 91 (2003) 216601.
- [8] A.D. Giddings, et al., *Phys. Rev. Lett.* 94 (2005) 127202.
- [9] M. Bartošík, et al., *J. Phys.: Conf. Ser.* 61 (2007) 75–79.
- [10] <http://math.nist.gov/oomb/contrib/simulmag>.